Chemical Engineering Journal 291 (2016) 269–278

Contents lists available at ScienceDirect

Chemical Engineering Journal

journal homepage: www.elsevier.com/locate/cej

Membrane bioreactors for treatment of saline wastewater contaminated by hydrocarbons (diesel fuel): An experimental pilot plant case study

Giorgio Mannina, Alida Cosenza, Daniele Di Trapani, Marco Capodici *, Gaspare Viviani

Dipartimento di Ingegneria Civile, Ambientale, Aerospaziale, dei Materiali, Università di Palermo, Viale delle Scienze, Ed. 8, 90100 Palermo, Italy

HIGHLIGHTS

- A membrane bioreactor to treat synthetic shipboard slops was monitored.
- Autotrophic activity was affected by salinity and diesel fuel dosing.
- A high sludge viscosity was recorded and this factor reduced the sludge filterability.
- Irreversible cake deposition was the main fouling mechanism.
- The MBR was effective in terms of hydrocarbon removal.

GRAPHICAL ABSTRACT

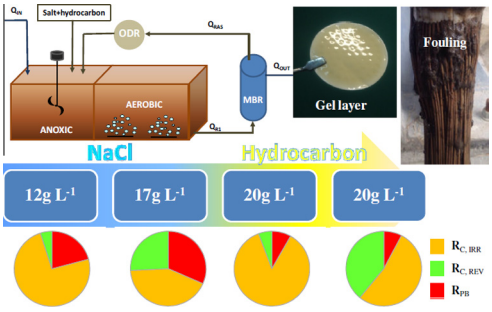

ARTICLE INFO

Article history:
Received 26 November 2015
Received in revised form 22 January 2016
Accepted 30 January 2016
Available online 15 February 2016

Keywords:
Shipboard slops
Salinity
Membrane fouling
Biomass kinetics

ABSTRACT

The paper reports the main results of an experimental campaign performed on a membrane bioreactor pilot plant designed to treat synthetic shipboard slops. The experimental campaign was divided into two phases: salinity acclimation up to 20 g NaCl L^{-1} (Phase I) and hydrocarbon (diesel fuel) dosing (Phase II). The observed results show that the carbon removal was not severely affected by the wastewater features. Conversely, respirometric tests showed that nitrification was strongly affected by the salinity (33% of nitrification efficiency at 20 g NaCl L^{-1} – Phase I) as a result of the salinity in the autotrophic biomass. Moreover, the sludge viscosity increased during Phase II due to the wastewater composition, leading to an increase in the membrane resistance, and severe degradation of the sludge dewaterability was also observed. Indeed, the capillary suction time increased by a factor of 3 times compared with that of Phase I.

1. Introduction

The International Convention for the Prevention of Pollution from Ships (MARPOL 1973) regulates wastewater treatment generated from ships and was modified by the protocol of 1978. The main aim of (1973) is to preserve the marine environment through complete elimination of pollution by oil and other harmful substances. In this context, MARPOL (1973) also focuses attention on the wastewater generated by washing oil tanks (bilge water or slops). The core features of these types of wastewater are high salinity and high content of organic matter, which is usually recalcitrant and slowly biodegradable [1,2]. Consequently, proper treatment of such wastewaters is crucial because they can contribute to the release and accumulation of xenobiotic compounds in the environment. Meeting the discharge limits for treatment of such wastewaters can be challenging with respect to dissolved organic matter, hydrocarbons and heavy metals (MARPOL, 1973).

These types of wastewater can be treated using either physical–chemical or biological systems. Although physical–chemical methods have been successfully applied in the past [3], they create several issues with respect to chemical consumption, high energy

* Corresponding author. Tel.: +39 0916657755; fax: +39 091 23860810.
E-mail address: marco.capodici@unipa.it (M. Capodici).

http://dx.doi.org/10.1016/j.cej.2016.01.107
1385-8947/

requirements and secondary pollution. Conversely, in recent years, the technical community has put forward many efforts toward the use of biological processes for treatment of wastewater to overcome the drawbacks of the physical–chemical processes. Among the biological processes, membrane bioreactors (MBRs) have emerged as an option for saline wastewater treatment [4,5]. MBRs can significantly improve the efficiency of pollutant removal compared with conventional activated sludge (CAS) processes and feature high-quality effluent, a small footprint and low sludge production rates. Therefore, MBRs have been proposed for treatment of saline waters contaminated by "xenobiotic and recalcitrant" compounds derived from shipboard activities, such as petroleum hydrocarbons [6]. However, due to the particular features (high salinity and organic matter content) of slops, several issues related to their biological treatment are still unknown or have been minimally investigated: (i) ability of conventional biomass to survive in extreme salinity conditions, (ii) ability of microorganisms to degrade oil, (iii) influence of microbial community characteristics on membrane fouling, and (iv) plant performance in treating a combination of slops and urban wastewater.

Among the aforementioned issues, the ability of the biomass to survive in extreme salinity conditions has been frequently investigated. Indeed, Johir et al. [4] investigated the effect of gradual variation of the salinity in an MBR system and observed a decrease of the dissolved organic carbon and ammonia uptake rate due to an inhibitory effect caused by the salinity. Similarly, Jang et al. [7] found a decrease of ammonia removal and an increase of membrane fouling during treatment of high salinity wastewater due to the particular microbial community features. Quite recently, Di Trapani et al. [5] compared the performance of a moving-bed membrane bioreactor and a MBR system subjected to a gradual increase of salinity (up to 10 g NaCl L^{-1}). Di Trapani and coworkers showed that both systems allowed a notably high efficiency in terms of carbon and ammonium removal under a gradual increase of salinity, and for the MBR system, they found an increase in pore fouling with salinity.

Despite such studies, investigations using MBR for saline and hydrocarbon wastewater treatment have been rarely undertaken thus far.

Moreover, as far as authors are aware, the combined effect of salinity (20 g NaCl L^{-1}) and hydrocarbons (20 mg TPH L^{-1}) during the treatment of shipboard slop with a MBR system has never been investigated in the technical literature. Bearing in mind these considerations, the aim of this paper is to explore the possibility of treating saline wastewater contaminated by hydrocarbons using MBR systems. In particular, an MBR pilot plant was set up and fed with a mixture of real and synthetic wastewater. The pilot plant was inoculated with a non-halophilic biomass previously acclimated to a moderate saline environment (10 g NaCl L^{-1}). The effect of the feeding salt rate (weekly increased up to 20 g NaCl L^{-1} with the focus to investigate the short term period biomass reaction) and hydrocarbons (20 mg TPH L^{-1}) was investigated in terms of organic carbon and nitrogen removal, biomass respiratory activity, sludge features (i.e., dewaterability) and membrane fouling tendency.

2. Materials and methods

2.1. Pilot plant and sampling campaign

The MBR pilot plant (Fig. 1) was built at the Laboratory of Environmental and Sanitary Engineering of Palermo University. The plant consisted of a feeding tank (volume of 320 L) in which real domestic wastewater was stored, and two reactors in series, one anoxic (volume 45 L) and one aerobic (volume 224 L), according to a pre-denitrification scheme. The MBR pilot plant hydraulic retention time (HRT) was set at 16 h. Salt and hydrocarbons were directly added into the anoxic tank. The solid–liquid separation was performed via an ultrafiltration (UF) hollow-fiber membrane module (Zenon Zeeweed, ZW 10, with specific area equal to 0.98 m^2 and a nominal porosity of 0.04 μm). An oxygen depletion reactor (ODR) was installed to ensure anoxic conditions inside the anoxic reactor despite the intensive aeration in the aerobic tank (Fig. 1). Permeate extraction (Q_{OUT}) was imposed at 20 L h^{-1}. The MBR pilot plant was started up with activated sludge characterized by a Mixed Liquor Suspended Solids (MLSS) concentration of 4000 mg L^{-1} previously acclimated at a salinity concentration of 10 g NaCl L^{-1}. The experimental campaign lasted 90 days and was divided into two phases: (i) acclimation to an increasing feeding salt rate lasting 30 days (Phase I), and (ii) constant feeding salt rate (20 g NaCl L^{-1}) and hydrocarbon dosage lasting 60 days (Phase II). More specifically, during Phase I, the biomass was acclimated to salinity by gradually increasing the salt concentration in the influent from 10 g NaCl L^{-1} to 20 g NaCl L^{-1}. During Phase II, hydrocarbons measured as total petroleum hydrocarbons (TPH) were dosed at a concentration of 20 mg TPH L^{-1} in the form of diesel fuel. Briefly, the added diesel fuel was composed by a hydrocarbon mixture comprising the semi-volatile fraction ranging from C10 to C30 and including species with even as well as odd number of carbon atoms (typical Diesel range organic (DRO) mix). The hydrocarbon concentration and the maximum threshold of salinity (20 g NaCl L^{-1}) were chosen to simulate a shipboard slop already subjected to physical–chemical pre-treatment.

The membrane was periodically backwashed (every 9 min for a period of 1 min) by pumping a fraction of the permeate back through the membrane module. Table 1 summarizes the main wastewater characteristics and the operational parameters.

During pilot plant operation, the influent wastewater, mixed liquor inside the biological tanks (anoxic and aerobic) and effluent permeate were sampled and analyzed for total and volatile suspended solids (TSS and VSS), total chemical oxygen demand (COD_{TOT}), supernatant COD (COD_{SUP}) ammonium nitrogen (NH_4-N), nitrite nitrogen (NO_2-N), nitrate nitrogen (NO_3-N), total nitrogen (TN), phosphate (PO_4-P), total carbon (TC) and inert carbon (IC). All analyses were performed according to the standard methods [8]. TPH was measured on extracted and evaporated samples. An AGILENT 6890 GC-FID system with auto-sampler and a Parker gas generator 9090 for hydrogen supply was adopted.

The pilot plant performance was evaluated in terms of COD removal, nitrification/denitrification efficiency, total nitrogen removal and TPH removal. More specifically, to single out the removal effect of the biological processes and filtration provided by the membrane, two different removal efficiencies were calculated [5]: the biological removal efficiency and the total removal efficiency. The biological removal efficiency was calculated as the difference between the COD_{TOT} value in the influent and the COD_{SUP} measured in the supernatant of mixed liquor samples (filtered at 0.45 μm) withdrawn from the MBR tank. The total COD removal efficiency (including also the removal effect of the membrane filtration) was assessed as the difference between the influent COD_{TOT} and the COD_{TOT} measured in the permeate samples.

The nitrification (η_{nit}), denitrification (η_{denit}) and nitrogen (η_{total}) removal efficiencies were evaluated as follows [9]:

$$\eta_{nit}(\%) = \frac{(NH_4^+\text{-}N_{in}) - (NH_4^+\text{-}N_{out}) - N_{assimilation}}{(NH_4^+\text{-}N_{in}) - N_{assimilation}}. \quad (1)$$

$$\eta_{denit}(\%) = \frac{(NH_4^+\text{-}N_{in}) + (NO_X\text{-}N_{in}) - (NH_4^+\text{-}N_{out}) - N_{assimilation} - (NO_X\text{-}N_{out})}{(NH_4^+\text{-}N_{in}) + (NO_X\text{-}N_{in}) - N_{assimilation}} \quad (2)$$

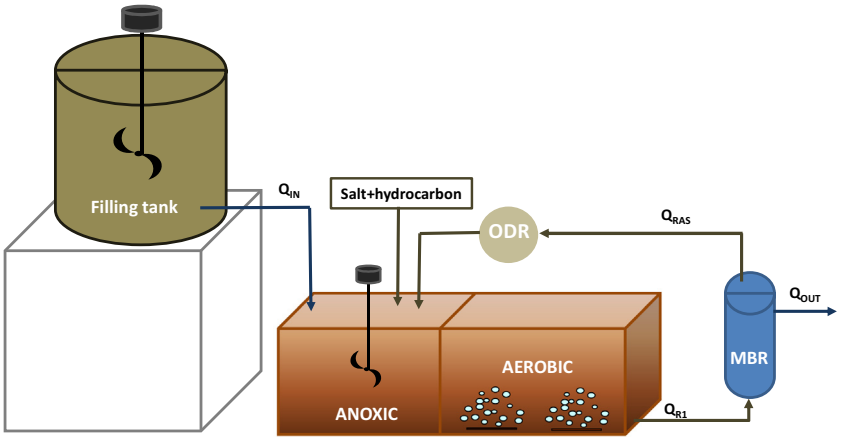

Fig. 1. Layout of the pilot plant (where Q_{IN} = influent wastewater; ODR = oxygen depletion reactor; MBR = membrane bioreactor; Q_{RAS} = recycled sludge from MBR to ODR; Q_{R1} = MLSS flow from aerobic tank to MBR).

Table 1
Main characteristics of the feed wastewater (average values) and operational conditions; *related only to Phase II (where HRT = hydraulic retention time).

Parameter	Unit	Value
COD	[mg L^{-1}]	350
TPH	[mg L^{-1}]	20*
NH_4-N	[mg L^{-1}]	50
PO_4-P	[mg L^{-1}]	6
NaCl	[mg L^{-1}]	10–20
Permeate flux	[L m^{-2} h^{-1}]	21
Flow rate	[L h^{-1}]	20
HRT	[h]	16

$$\eta_{total}(\%) = \frac{(NH_4^+\text{-}N_{in}) + (NO_X\text{-}N_{in}) - (NH_4^+\text{-}N_{out}) - (NO_X\text{-}N_{out})}{(NH_4^+\text{-}N_{in}) + (NO_X\text{-}N_{in})}. \quad (3)$$

where NH_4^+-N_{in} = influent nitrogen ammonia concentration, NH_4^+-N_{out} = permeate nitrogen ammonia concentration, $N_{assimilation}$ = -assimilated nitrogen (5% of the total BOD removed), NO_x-N_{in} = influent nitrite and nitrate concentration, and NO_x-N_{out} = permeate nitrite and nitrate concentration.

Finally, the TPH removal efficiency was assessed as the difference between the influent TPH and the TPH measured in the permeate samples.

2.2. Respirometric batch tests

Respirometric batch experiments were conducted using a "flowing gas/static-liquid" type as the batch respirometer [10]. The suspended biomass samples were collected from the bioreactors of both plants and diluted with permeate to obtain a mixed liquor concentration in the range of 2.0–3.0 g VSS L^{-1}. Before running the respirometric test, each sample was aerated until endogenous conditions were reached. For further details on the adopted procedure, the reader is referred to the literature [5]. In the batch tests designed to evaluate the heterotrophic biokinetic parameters, the nitrifying biomass was inhibited by adding 10–15 mg L^{-1} of Allylthiourea (ATU), and the exogenous oxygen uptake rate (OUR) was enhanced by the addition of a readily biodegradable organic substrate (sodium acetate in the current study). The substrate biodegradation rate was assumed proportional to the exogenous OUR, according to the following expression:

$$\Delta COD = \frac{\Delta O_2}{1 - f_{cv} \cdot Y_H} \quad (4)$$

where f_{cv} is the conversion coefficient from COD to VSS and assumed equal to 1.42 mg COD mg^{-1} VSS, and Y_H is the yield coefficient (mg VSS mg^{-1} COD). The yield coefficient Y_H was derived from the integral of the exogenous OUR chart according to the methodology suggested by [11]. The maximum heterotrophic growth rate $\mu_{H,max}$ (d^{-1}) and the half saturation coefficient KS (mg COD L^{-1}) were evaluated by solving the Monod-type kinetic expression with the finite difference procedure and fitting the following equation:

$$\frac{\Delta COD}{\Delta t} = \frac{\mu_{H,max}}{Y_H} \cdot \frac{COD}{(K_S + COD)} \cdot X_H \quad (5)$$

where COD is the carbonaceous substrate concentration at time t (mg L^{-1}), X_H is the biomass active fraction (mg VSS L^{-1}), and $\mu_{H,max}$ and K_S were previously defined. Estimation of the endogenous decay coefficient b_H and X_H were performed according to the "single batch test" procedure [5,12].

The kinetic parameters of autotrophic species were estimated using the same procedure. Nevertheless, in this case, no inhibiting substance such as ATU was added and ammonium chloride (NH_4-Cl) was directly spiked to evaluate the biokinetic parameters. The conversion factor between oxygen and ammonium (NOD: nitrogen oxygen demand) is equal to:

$$\Delta NH_4\text{-}N = \frac{\Delta O_2}{4.57}. \quad (6)$$

2.3. EPS analysis and extraction

Total extracellular polymeric substances (EPS_T) were measured using the thermal extraction method [13,14]. According to this method, the EPS_T are partitioned into two fractions: soluble microbial products (SMPs) and bound EPS (EPS_{Bound}). Both SMPs and EPS_{Bound} were fractionated into protein and carbohydrate compounds. The EPS_T was evaluated as the sum of proteins and carbohydrates compounds of SMPs and EPS_{Bound}:

$$EPS_T = \underbrace{EPS_P + EPS_C}_{EPS_{Bound}} + \underbrace{SMP_P + SMP_C}_{SMP} \quad (7)$$

where the subscripts P and C indicate the content of proteins and carbohydrates in the EPS_{Bound} and SMP, respectively.

Carbohydrates in the EPS_T were determined according to the phenol–sulfuric acid method with glucose as the standard [15]. Proteins were determined by the Folin method as proposed by [16]. For further details, reader is referred to the literature [13].

2.4. Resistance analyses

The total resistance (R_T) to membrane filtration was evaluated using Darcy's law:

$$R_T = \frac{\mathrm{TMP}}{\mu \mathrm{J}} \tag{8}$$

where TMP is the transmembrane pressure (Pa), μ is the permeate viscosity (Pa s), and J is the permeation flux ($\mathrm{m\,s^{-1}}$).

During membrane filtration, R_T can be evaluated as the sum of the intrinsic resistance of membrane (R_m) and the resistance due to membrane fouling (R_F):

$$R_T = R_m + R_F \tag{9}$$

The membrane fouling (R_F) can be fractionated as follows:

$$R_F = R_{\mathrm{PB}} + R_{\mathrm{C,irr}} + R_{\mathrm{C,rev}} = R_T - R_m \tag{10}$$

where R_{PB} is the irreversible resistance due to colloid and particle deposition in the membrane pores, $R_{\mathrm{C,irr}}$ is the fouling resistance related to superficial cake deposition that can be only removed by physical cleaning (hydraulic/sponge scrubbing), and $R_{\mathrm{C,rev}}$ is the fouling resistance related to superficial cake deposition that can be removed by ordinary backwashing.

The specific fouling mechanism was studied by applying the resistance in-series method [5].

To limit the total resistance with respect to a fixed threshold value, physical membrane cleaning was performed according to [17]. Specifically, during physical cleaning, the membrane module was removed from the reactor and washed with ultrapure water to remove the cake layer on the membrane surface. The washed membrane module was placed in a tank with ultrapure water, and the TMP and J were monitored; thus, the total resistance (R_{T1}) was evaluated. The washed module was submerged into the mixed liquor, the TMP and J were monitored, and the resistance after physical cleaning (R_{T2}) was evaluated.

Consequently R_{T1} and R_{T2} can be fractionated as:

$$R_{T1} = R_m + R_{\mathrm{PB}} \tag{11}$$

$$R_{T2} = R_m + R_{\mathrm{PB}} + R_{C,\mathrm{rev}} \tag{12}$$

Thus, each fouling resistance fraction was evaluated as:

$$\begin{cases} R_{\mathrm{PB}} = R_{T1} - R_m & (13) \\ R_{\mathrm{C,rev}} = R_{T2} - R_{T1} & (14) \\ R_{\mathrm{C,irr}} = R_T - R_{T1} - R_{\mathrm{C,rev}} & (15) \end{cases}$$

Furthermore, chemical cleaning processes were also performed to reduce the R_{PB} value.

More precisely, after physical cleaning, the washed module was placed in a tank with clean water containing 2 g $\mathrm{L^{-1}}$ of citric acid ($C_6H_8O_7$) at a temperature of 40 °C for 4 h. The washed module was submerged in a tank with ultrapure water, the TMP and J were monitored, and the resistance was evaluated after chemical cleaning ($R_{T1,\mathrm{CC}}$). The amount of R_{PB} removed by the chemical cleaning was evaluated as:

$$R_{T1} - R_{T1,\mathrm{CC}} \tag{16}$$

2.5. Sludge dewaterability

The capillary suction time (CST) and the specific resistance to filtration (SRF) were measured to investigate the sludge dewaterability features [18–20]. The CST and SFR were measured in accordance with [21,22] by analyzing fresh samples collected from the aerobic tank. In detail, the CST measurements were determined by pouring a volume of sample into a sludge reservoir placed on Whatman No. 17 filter paper. An electronic device recorded the time necessary for the filtrate to cover the space between two probes, which detected the advancement of the liquid front on the paper. The CST was assessed as the average value of three replicates. The SRF was evaluated in the reduced pressure condition (−50 kPa). In detail, the vacuum condition was applied by a vacuum pump connected to a Buchner funnel in which Whatman 41 (20 μm pore size) filter paper was placed. After pouring 100 of sample on the funnel, the filtrate volumes (V) and the corresponding time (t) were recorded. The SRF was calculated in accordance with Eq. (17):

$$r = \frac{2 \cdot \Delta p \cdot A^2 \cdot b}{\mu \cdot C_0} \tag{17}$$

where Δp is the pressure drop across the filter, A is the filtration area, μ is the viscosity of filtrate at the temperature of the sludge, b is the slope of the linear portion of the curve obtained by plotting t/V versus V, and C_0 is the initial dry residue of the sludge.

The viscosity of filtrate was measured using a Brookfield rotational viscometer. In details, 16 ml of mixed liquor, derived from the aerobic tank, were put into a metallic cylindrical shaped vessel where the sludge temperature was controlled (20 °C ± 0.1 °C) by means of a thermostat. The rotor velocity was set equal to 60 rpm and the corresponding viscosity value was expressed in cP.

3. Results and discussion

3.1. Organic and nitrogen removal

Table 2 reports the main results in terms of average performance during the two phases of the experimental campaign. Fig. 2 shows data related to the influent and effluent COD (a) and NH_4-N (b); Fig. 2a also reports data of the supernatant COD in MBR tank.

The MBR pilot plant showed a reduction in biological COD removal (from 87% to 63%) with the increase of the feeding salt rate (Table 2; Fig. 2a). Moreover, the lowest reduction of the biological COD removal occurred at 20 g NaCl $\mathrm{L^{-1}}$ (namely, 63%) (Table 2, Fig. 2a). This result could be due to a partial inhibition effect exerted by the high salinity (20 g NaCl $\mathrm{L^{-1}}$) on the heterotrophic species.

In terms of total COD removal, the MBR pilot plant exhibited notably high performance throughout the experiments, with an average value close to 90%. In particular, when the feeding salt rate was increased from 14 g NaCl $\mathrm{L^{-1}}$ to 17 g NaCl $\mathrm{L^{-1}}$, the total COD removal efficiency was greater than 96% (on average). Such a result confirmed the effectiveness and the robustness of the MBR systems even in the presence of high salinity [7,23]. However, increasing the feeding salt rate up to 20 g NaCl $\mathrm{L^{-1}}$ created a reduction of the biological performance and a total COD decrease (down to 75%) (Table 2). Nevertheless, during Phase II (20 g NaCl $\mathrm{L^{-1}}$ and 20 mg TPH $\mathrm{L^{-1}}$), the MBR pilot plant showed overall good performance in removal (i.e., total COD removal equal to 91%). Such a result can be explained by acknowledging the key role played by the physical membrane. Indeed, the physical membrane compensated for the reduction of the biological efficiency (average value 64%) caused by the inhibitory effect exerted by the salinity and hydrocarbons.

In terms of TPH removal, a high removal efficiency (namely, 88%) was obtained during the experimental period. However, it is important to note that during the first days of Phase II (namely, between days 30–43), the TPH removal efficiency was quite low with an average value equal to 50%. This result highlights the initial inability of biomass to remove the TPH. Thus, the results suggest

Table 2
Average biological performance in terms of COD, N, nitrification, denitrification and TPH removal.

		Phase I				Phase II
		12 gNaCL L^{-1}	14 gNaCL L^{-1}	17 gNaCL L^{-1}	20 gNaCL L^{-1}	20 g NaCL L^{-1} + 20 mg TPH L^{-1}
Biological COD removal	[%]	87	81	79	63	64
Total COD removal	[%]	96	97	95	75	91
η_{nit}	[%]	83	74	63	33	39
η_{denit}	[%]	0	54	47	26	20
η_{Ntotal}	[%]	52	73	73	42	53
TPH removal	[%]	–	–	–	–	88

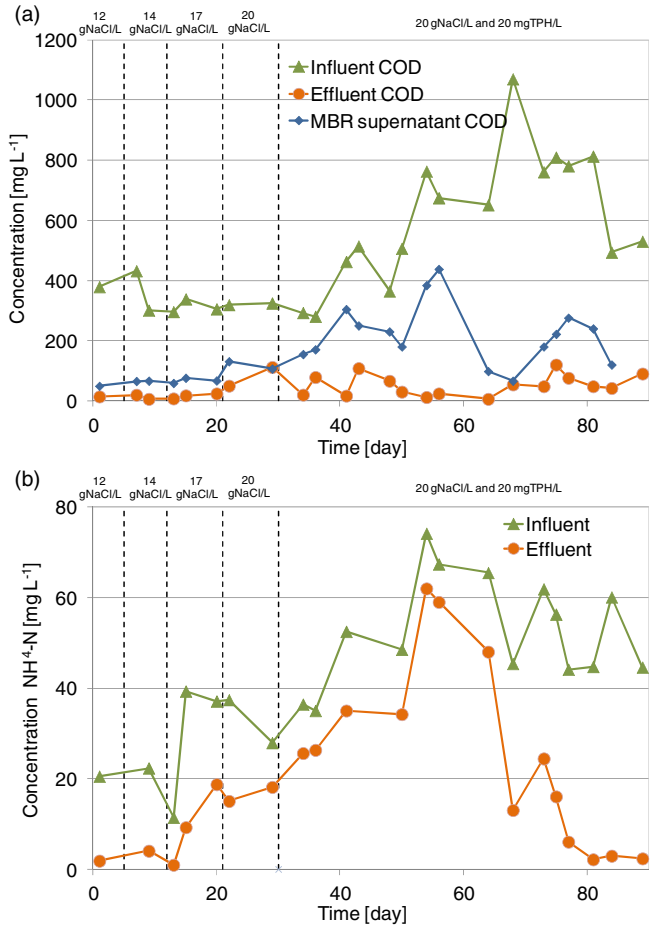

Fig. 2. Influent, MBR supernatant and effluent COD concentrations (a); influent and effluent ammonia concentrations (b), respectively.

that to obtain good plant performance in terms of TPH removal, a gradual and moderate increase of the TPH feeding rate (up to the design value) should be used to enhance biomass acclimation to the hydrocarbon content [24]. However, according to the overall TPH removal, we can conclude that MBRs are a promising technology for treating oily wastewater results.

The nitrification process was strongly influenced by the salinity. Indeed, the nitrification efficiency ranged from 33% to 83% (Table 2). A shock effect on the autotrophic species was recorded due to the salt rate (approximately 14 g NaCl L^{-1}), which ended near the 67th day (as better outlined in the following). The lowest ammonia nitrification efficiency (33%) was obtained at the highest salinity level (20 g NaCl L^{-1}), thus indicating the harmful effect of the salinity on nitrification. Such a result is in agreement with the literature, which suggests that nitrifiers are highly sensitive to salinity variation [25,26].

Fig. 3a shows the NO_2-N and NO_3-N in the aerobic reactor. It is possible to notice a NO_2-N accumulation (from 0.5 mg/L to 8 mg/L) in the aerobic reactor for a feeding salt rate ranging from 12 to 17 g NaCl L^{-1} (Fig. 3a). Such a result highlights that the *nitrite oxidizing bacteria* (NOB) activity was severely affected by the salinity variation, confirming that NOB microorganisms are highly sensitive to the feeding salt rate. When the feeding salt rate was increased to 20 g NaCl L^{-1}, both *ammonia oxidizing bacteria* (AOB) and NOB species were severely inhibited, and the NO_3-N and the NO_2-N concentrations inside the aerobic reactor collapsed to zero (Fig. 3a). Therefore, a feeding salt rate of 20 g NaCl L^{-1} represented a threshold value that produced a significant stress effect on the autotrophic species. Moreover, the hydrocarbon dosage might have contributed to a further inhibition of nitrifier activity, as also confirmed by the respirometric batch tests. Indeed, following the

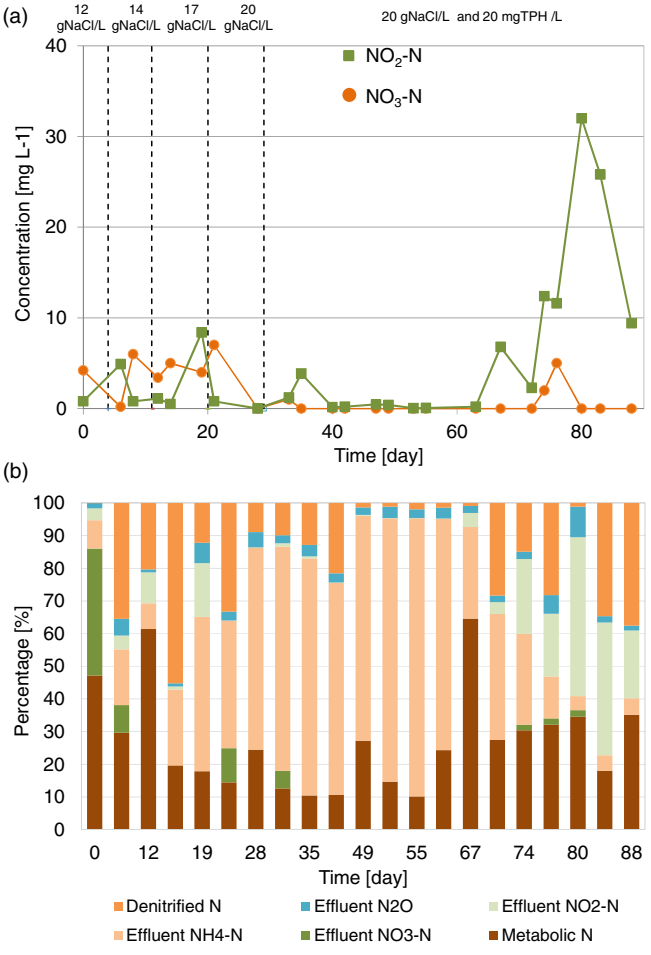

Fig. 3. NO_2-N and NO_3-N concentration in the aerobic tank (a) and nitrogen forms as a percentage of the total nitrogen (b), respectively.

hydrocarbon addition, NO_3-N and NO_2-N concentrations inside the aerobic tank were negligible until the 63rd experimental day, highlighting a complete inhibition of both AOB and NOB species (Fig. 3a). Nevertheless, after the 67th experimental day, NO_2-N accumulation was observed, whereas the NO_3-N production remained quite negligible, thus suggesting a partial recovery of the AOB species activity. Conversely, the NOB species were still inhibited by the high saline environment (Fig. 3a). Therefore, it can be suggested that longer durations are required to restore the full nitrification ability. This result was also confirmed by the balance of nitrogen forms (Fig. 3b). Indeed, from the analysis of Fig. 3b, it is worth noting the predominance of the effluent NH_4-N at the end of Phase I (20 g NaCl L^{-1}) and during Phase II (20 g NaCl L^{-1} and hydrocarbon dosage), whereas the effluent NO_2-N and NO_3-N were nearly negligible. Conversely, after the 67th experimental day, a significant decrease of the effluent ammonia was observed, corresponding to an increase of the effluent nitrite due to the recovery of AOB activity.

This condition is likely to have influenced the denitrification efficiency, which remained quite low (ranging from 0% to 54%). Indeed, the denitrification efficiency decreased through time as a result of the salt rate increase. During the second phase, which was characterized by the highest salt rate and hydrocarbon dosage, the denitrification efficiency collapsed to nearly zero. However, after the 67th day, an increase of the denitrification efficiency was observed as a consequence of the recovery of AOB activity. Moreover, the low denitrification efficiency was likely influenced by the inability to maintain constant and null dissolved oxygen concentrations inside the anoxic tank.

Finally, the negative effects exerted by the salinity and hydrocarbons on the nitrification/denitrification processes contributed to the low efficiency in terms of TN removal. In particular, at the end of Phase I (feeding salt rate of 20 g NaCl L^{-1}) and during Phase II (feeding salt rate of 20 g NaCl L^{-1} and hydrocarbon dosage), the average removal efficiencies were equal to 42% and 53%, respectively.

3.2. Biokinetic behavior

The evaluation of biomass activity during experiments in terms of kinetic and stoichiometric parameters of both heterotrophic and autotrophic species was assessed via respirometry. Referring to heterotrophic activity, Fig. 4a reports the trend of the specific oxygen uptake rate (SOUR). It is possible to note a significant decrease of biomass respiration rates (Fig. 4a). This result was likely due to a stress effect related to the presence of hydrocarbons in the inlet wastewater. Nevertheless, it is worth mentioning that the SOUR decrease was delayed compared with the starting day of hydrocarbon dosage, thus suggesting that worsening of heterotrophic activity could be due to the accumulation of hydrocarbons inside the system. Moreover, the heterotrophic biomass showed a "storage" phenomenon, which is typical of systems subjected to dynamic conditions. Such a condition likely enhanced the growth of bacterial groups able to rapidly convert the organic substrate into storage products. The storage yield coefficient Y_{STO} was evaluated according to the procedure proposed by [27].

Referring to autotrophic species, a different behavior was observed compared with that of heterotrophs. Indeed, starting from a feeding salt rate of 14 g NaCl L^{-1}, a significant inhibition of autotrophic species was observed due to the effect of salinity (Fig. 4b). Previous studies highlighted that autotrophic species are highly sensitive to salt variations [5]. However, after the 45th experimental day, a slight increase of autotrophic growth rates was noted, indicating recovery of the nitrification. Such a result was likely related to the acclimation of autotrophic species, suggesting that in the long term, it is possible to restore the good nitrification capability of the system, even in the presence of a high feeding salt rate and the presence of petroleum hydrocarbons, as in the inlet wastewater. Table 3 summarizes the obtained stoichiometric/kinetic parameters during the experiments. In general, from the analysis of Table 3, it is possible to observe a slight decrease of kinetic/stoichiometric parameters compared with the values in the technical literature.

3.3. Salt and hydrocarbon effects on membrane filtration

Fig. 5 reports the fouling trend in terms of total resistance (R_T) (Fig. 5a) and resistance decomposition according to Eq. (10) (Fig. 5b). Furthermore, the percentage contribution of each resistance (calculated as the ratio of the fouling resistance) during certain representative plant operational days is reported (Fig. 5c1–c4). As shown in Fig. 5a, over the entire experimental period, ten membrane cleaning operations were performed. In particular, eight physical and two chemical cleanings were performed. The membrane cleaning operations were intended to prevent the TMP from exceeding the critical values defined by the membrane manufacturer (namely, 0.5–0.6 bar). Furthermore, at the 28th day, the membrane was damaged and was replaced by a new identical one.

Hydrocarbon dosing led to a rapid degradation of the membrane filtration properties (Fig. 5a). Indeed, the average R_T value of Phase II (namely, $9.9{\cdot}10^{12}$ m^{-1}) was twice that of Phase I (namely, $5.02{\cdot}10^{12}$ m^{-1}) (Fig. 5a). The irreversible resistance due to superficial cake layer ($R_{C,irr}$) represented the highest fraction of the total hydraulic resistance to filtration (Fig. 5b). Furthermore, during Phase II, even the contribution of the reversible resistance due to the superficial cake layer ($R_{C,rev}$) increased. At the end of Phase I, the $R_{C,rev}$ was equal to the 22% of the total resistance (R_T) (Fig. 5c2), and during Phase II, it increased up to 39% (Fig. 5c4).

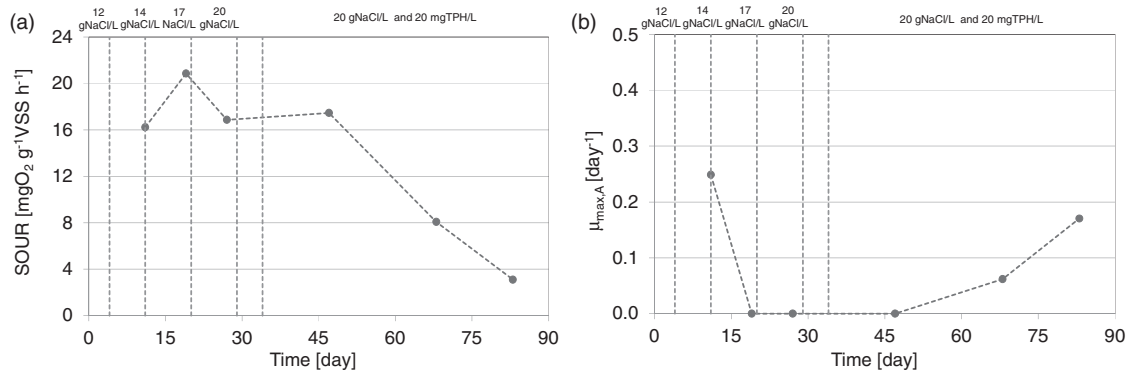

Fig. 4. Specific respiration rates of heterotrophic species (a), and maximum growth rates for autotrophic species (b).

Table 3
Average values of kinetic and stoichiometric parameters during experiments (standard deviation is given in brackets).

	Salinity [10–20 g NaCl L^{-1}]	Salinity and hydrocarbons [20 g NaCl L^{-1}, 20 mg TPH L^{-1}]	Literature	Refs.
Heterotrophic				
Y_H [mg COD mg^{-1} COD]	0.59 (±0.012)	0.70 (±0.12)	0.67	[28]
Y_{STO} [mg COD mg^{-1} COD]	0.79 (±0.013)	0.78 (±0.09)	0.78	[27]
$\mu_{H,max}$ [d^{-1}]	5.07 (±0.53)	3.58 (±0.96)	6	[28]
K_S [mg COD L^{-1}]	4.21 (±0.81)	4.22 (±1.36)	20	[28]
$SOUR_{max}$ [mg O_2 g^{-1} TSS h^{-1}]	17.99 (±2.5)	9.55 (±7.29)	–	–
Autotrophic				
Y_A [mg COD mg^{-1} N]	0.14 (±0.24)	0.26 (±0.06)	0.24	[29]
$\mu_{A,max}$ [d^{-1}]	0.12 (±0.18)	0.12 (±0.08)	0.8	[28]
K_{NH} [mg NH_4-N L^{-1}]	0.24 (±0.42)	0.65 (±0.50)	1.00	[28]
Nitrif. rate [mg NH_4-N L^{-1} h^{-1}]	0.39 (±0.67)	1.12 (±0.86)	2.30	[30]

Y_H = heterotrophic yield coefficient, Y_{STO} = storage yield coefficient, $\mu_{H,max}$ = maximum heterotrophic growth rate, K_S = heterotrophic half-saturation coefficient, $SOUR_{max}$ = specific respiration rate, Y_A = autotrophic yield coefficient, $\mu_{A,max}$ = maximum autotrophic growth rate, K_{NH} = autotrophic half-saturation coefficient.

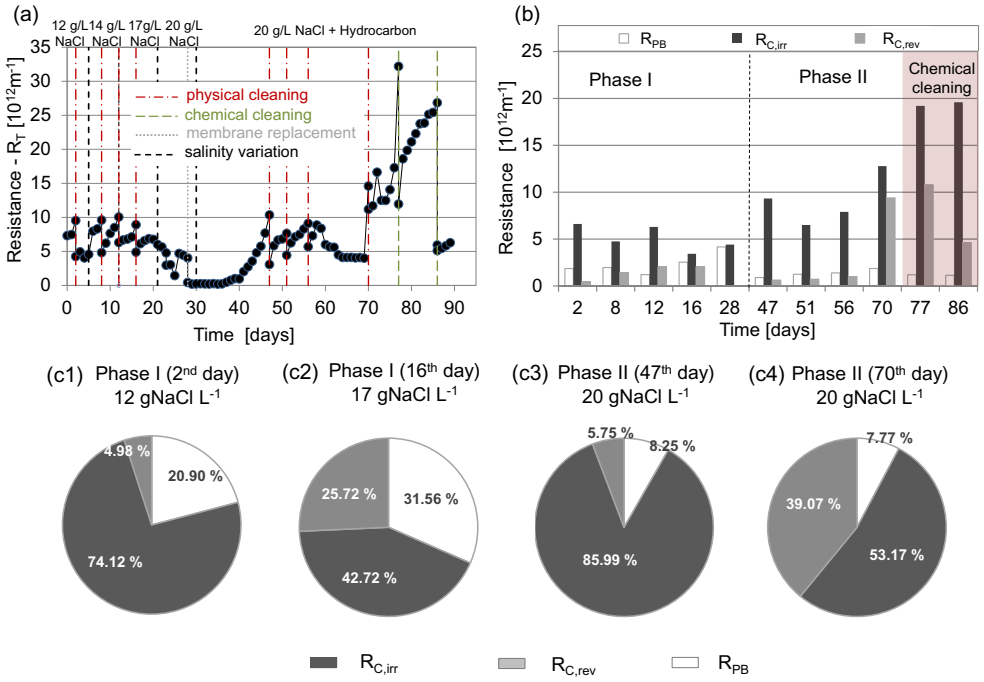

Fig. 5. Total R_T (a), specific resistances (b), and percentage of each resistance fraction with respect to the total fouling resistance (c).

The increase of the $R_{C,rev}$ resistance occurred during both Phase I and II (Fig. 5c1–c4). The high values of both $R_{C,irr}$ and $R_{C,rev}$ compared with R_{PB} during Phase II were likely due to worsening of the sludge properties (high viscosity). Indeed, during Phase II, the average sludge viscosity increased from 3.5 cP (Phase I) up to 5 cP (Phase II). The literature demonstrates that the sludge viscosity is positively correlated with the cake layer formation [31–34]. Therefore, in this study, the increase of sludge viscosity significantly influenced the resistance due to the cake ($R_{C,irr}$ and $R_{C,rev}$) [33]. The increase of sludge viscosity was most likely due to the hydrocarbon dosing in a salt environment (salinity rate of 20 g NaCl L^{-1}). However, in contrast with previous literature studies that show a sludge viscosity increase with EPS_T, our findings revealed an opposite trend, i.e., the average EPS_T (inside the aerobic tank) decreased from 210 mg EPS g^{-1} TSS (Phase I) to 124 mg EPS g^{-1} TSS (Phase II). Such a result could be likely due to a deflocculation effect of the sludge flocs as a result of the operational conditions due to the salinity and toxic compounds (i.e., hydrocarbon) (Li et al. [32]). As a matter of a fact, the average SMP concentration inside the aerobic tank increased from 2.7 mg EPS g^{-1} TSS (Phase I) up to 13.6 mg EPS g^{-1} TSS (Phase II). The increase of SMP is recognized as important evidence of sludge deflocculation, thus corroborating our hypothesis [35].

The SMP concentration inside the aerobic tank strongly influenced the membrane fouling. A rather high correlation exists between the SMP concentration inside the aerobic tank and R_T (R^2 = 0.82) (Fig. 6a). Indeed, as confirmed by the technical literature, due to their low dimension (50–500 kDa), SMPs are often responsible for membrane fouling [34]. However, in terms of EPS_{Bound}, an opposite correlation was found with R_T (Fig. 6b). Indeed, the R_T value increased with the decrease of EPS_{Bound}. A similar result was obtained by correlating $EPS_{Bound,C}$ with $R_{C,irr}$ (Fig. 6c). This finding is in line with previous studies demonstrating that worsening of the sludge features (viscous and "bloated" sludge) produced a cake layer characterized by low resistance and a reduction of the pre-filter effect exerted by the cake layer [24,36,37]. Indeed, as discussed above, the reduction of EPS_{Bound} caused a loss of the stability of sludge flocs (deflocculation) leading to a cake

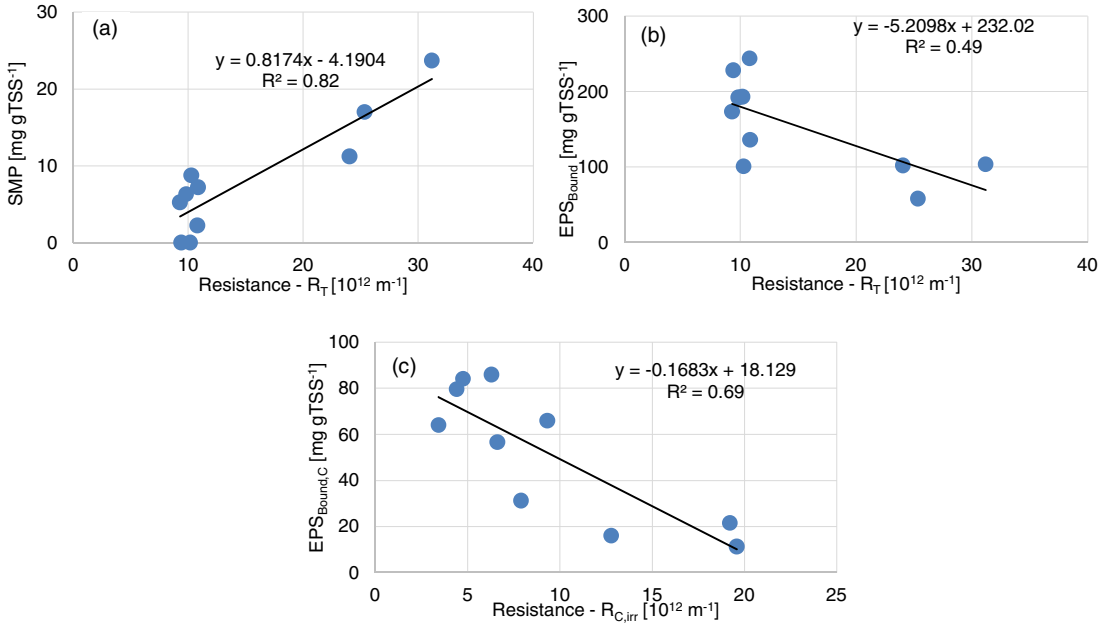

Fig. 6. Correlation between SMP and R_T (a), between EPS_{Bound} and R_T (b), and between $EPS_{Bound,C}$ and $R_{C,irr}$ (c).

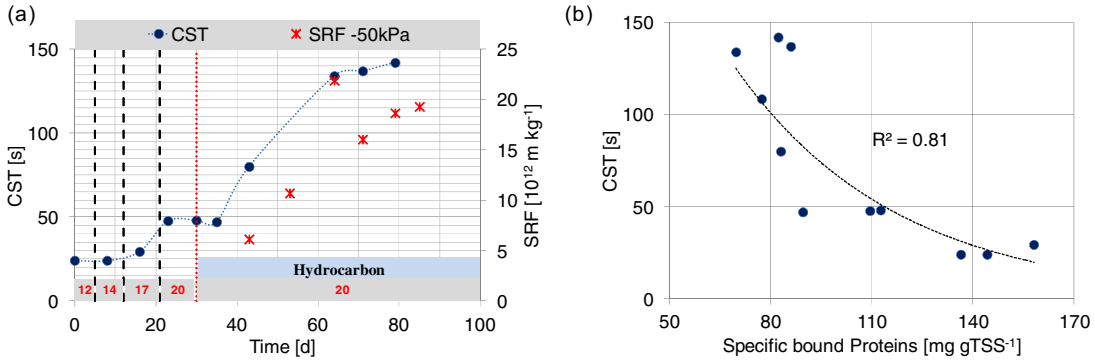

Fig. 7. CST and SRF measures (a) and correlation between CST and specific bound EPS fraction (b).

layer characterized by particles of small dimensions, which in turn increased the fraction of $R_{C,irr}$. Furthermore, the reduction of EPS_{Bound} led to an increase of SMP concentration that could more easily reach the membrane pores, thus contributing to the increase in the total resistance to filtration.

3.4. Sludge dewaterability

The main results of sludge analysis for dewaterability features are shown in Fig. 7.

The results reported in Fig. 7a show that up to 17 g NaCl L^{-1}, the step-wise salinity increase exerted a significant effect on CST and thus on sludge dewaterability. Indeed, the CST value measured at 12 and 14 g NaCl L^{-1} was nearly constant (namely, 24 s). Conversely, when the salinity was increased up to 17 g NaCl L^{-1}, the measured CST increased up to 29.33 s. Furthermore, at a salinity of 20 g NaCl L^{-1}, the dewaterability of the aerobic sludge significantly worsened. Indeed, the CST values were almost twice the values measured at 12 and 14 g NaCl L^{-1}. This result is in line with literature and shows how the stress condition exerted by the step-wise salinity increase affected the sludge dewatering [38]. Raynaud and coworker [38] found that the addition of NaCl in activated sludge leads to a longer time for dewatering and also suggested that the addition of NaCl leads to a release of fine particles that are assumed to clog the filter medium, thus limiting the flow throughout the porous system. During Phase II, the hydrocarbon dosing led to a considerable increase of the CST. Indeed, from the 30th to the 79th day, the CST value constantly increased up to a maximum value (namely, 142 s). Such a value is nearly 6 times higher than values related to a salt rate of 12–14 g NaCl L^{-1}. The SRF measurements (right axis of Fig. 7a) provided similar results, thus corroborating the CST findings with respect to the progressive decrease of sludge filterability during Phase II. During Phase II, sludge filtering operations encountered increasing difficulty. More specifically because the beginning of hydrocarbon dosing, the sample collected from the MBR pilot plant showed a progressive decrease in filterability, causing a longer duration of the vacuum pump operations needed to collect significant volumes of filtered sample. Furthermore, after filtration, the filtration media was covered by a homogeneous jelly layer.

This result was likely ascribable to the progressive increase in sludge viscosity, primarily due to worsening of the bacterial consortium features. Li and Yang [39] found that the difficulty in sludge dewatering increases with the increase in sludge viscosity and also suggested that the increase of the sludge viscosity is primarily related to an increase of loosely bound EPS. The effect of the bound fraction of EPS on dewatering was also noted in the current study. Fig. 7b shows the influence of specific bound protein

fraction of EPS on CST. The highest CST values corresponded with the lowest concentration of specific bound protein. It is worth noting that the role played by EPS in sludge dewaterability still remains controversial [40]. Indeed, [41,42] found that the sludge dewaterability initially increases with EPS content but subsequently decreases once the EPS content exceeds a threshold value. Conversely, other authors reported that the sludge dewaterability improves after the EPS reduction [43]. Furthermore, according to our findings, the presence of hydrocarbons characterized by high hydrophobicity could also have exerted a significant effect on sludge viscosity and thus on the dewatering phenomena, making comprehension of the results more difficult.

4. Conclusions

The current study explored the possibility of using MBR systems to treat saline wastewater contaminated by hydrocarbons. The MBR pilot plant produced high total COD removal efficiencies during experiments with an average value near 90%. However, the biological COD removal was affected by the feeding salt rate and the hydrocarbon addition, showing a significant reduction. The autotrophic activity was strongly limited due to the salinity increase and hydrocarbon dosing. A partial recovery of the autotrophic activity occurred at the end of the experimental period (Phase II), highlighting the slow acclimation capability of the autotrophic bacteria. As a result of the wastewater composition, the sludge viscosity greatly increased, causing membrane fouling issues with irreversible cake deposition as the main fouling mechanism. Furthermore, the high sludge viscosity led to a reduction of the sludge filterability. In the short term, such effects caused a reduction of the physical performance of the membrane. Therefore, to successfully apply MBRs for treatment of saline wastewater contaminated by hydrocarbons, it is crucial to extend the start-up period (enhancement of biomass acclimation) and explore the possibility of considering chemical addition to cope with sludge worsening and thus enhance membrane filtration. The use of chemicals could entail a notable increase of the operation costs. Thus, MBR option as a possible solution for treating saline and contaminated of hydrocarbon shipboard slops should be carefully assessed by a cost-benefit analysis.

Acknowledgments

This research was funded by the National Operational Programme for Research and Competitiveness 2007–2013. Project STI-TAM (Sviluppo di Tecnologie Innovative per il trattamento di rifiuti liquidi della navigazione finalizzate alla Tutela dell'Ambiente Marino) – PON 02_00153_2849085 – CUP B61C12000840005; Italian Ministry of Education, University and Research and Ministry of Economic Development. This work forms also part of a research project supported by grant of the Italian Ministry of Education, University and Research (MIUR) through the Research project of national interest PRIN2012 (D.M. 28 dicembre 2012 n. 957/Ric – Prot. 2012PTZAMC) entitled "Energy consumption and GreenHouse Gas (GHG) emissions in the wastewater treatment plants: a decision support system for planning and management – http://ghgfromwwtp.unipa.it" in which the first author is the Principal Investigator.

References

[1] C. Sun, T. Leiknes, J. Weitzenbock, B. Thorstensen, Development of a biofilm-MBR for shipboard wastewater treatment: the effect of process configuration, Desalination 250 (2010) 745–750.
[2] A.R. Pendashteh, C.A. Luqman, A. Fakhru'l-Razia, S.S. Madaeni, Z.A. Zainal, A.B. R. DayangRadiah, Evaluation of membrane bioreactor for hypersaline oily wastewater treatment, Process Saf. Environ. Prot. 90 (2012) 45–55.
[3] G. Li, S.H. Guo, F.M. Li, Treatment of oilfield produced water by anaerobic process coupled with micro-electrolysis, J. Environ. Sci. 22 (2010) 1875–1882.
[4] M.A.H. Johir, S. Vigneswaran, J. Kandasamy, R. BenAim, A. Grasmick, Effect of salt concentration on membrane bioreactor (MBR) performances: detailed organic characterization, Desalination 322 (2013) 13–20.
[5] D. Di Trapani, G. Di Bella, G. Mannina, M. Torregrossa, G. Viviani, Comparison between moving bed-membrane bioreactor (MB-MBR) and membrane bioreactor (MBR) systems: influence of wastewater salinity variation, Bioresour. Technol. 162 (2014) 60–69.
[6] S. Soltani, D. Mowla, M. Vossoughi, M. Hesampour, Experimental investigation of oily water treatment by membrane bioreactor, Desalination 250 (2010) 598–600.
[7] D. Jang, Y. Hwang, H. Shin, W. Lee, Effects of salinity on the characteristics of biomass and membrane fouling in membrane bioreactors, Bioresour. Technol. 141 (2013) 50–56.
[8] APHA, Standard Methods for the Examination of Water and Wastewater, APHA, AWWA and WPCF, Washington DC, USA, 2005.
[9] J. Wagner, L.B. Guimarães, T.R.V. Akaboci, R.H.R. Costa, Aerobic granular sludge technology and nitrogen removal for domestic wastewater treatment, Water Sci. Technol. 71 (7) (2015) 1040–1046.
[10] H. Spanjers, P.A. Vanrolleghem, G. Olsson, P. Dold, Respirometry in control of the activated sludge process, Water Sci. Technol. 34 (1996) 117–126.
[11] P.A. Vanrolleghem, H. Spanjers, B. Petersen, P. Ginestet, I. Takacs, Estimating (combination of) Activated Sludge Model No. 1 parameters and component by respirometry, Water Sci. Technol. 39 (1999) 195–214.
[12] A. Ramdani, P. Dold, S. Deleris, D. Lamarre, A. Gadbois, Y. Comeau, Biodegradation of the endogenous residue of activated sludge, Water Res. 44 (2010) 2179–2188.
[13] A. Cosenza, G. Di Bella, G. Mannina, M. Torregrossa, G. Viviani, Biological nutrient removal and fouling phenomena in a University of Cape Town membrane bioreactor treating high nitrogen loads, J. Environ. Eng. 139 (2013) 773–780.
[14] A. Cosenza, G. Di Bella, G. Mannina, M. Torregrossa, G. Viviani, The role of EPS in fouling and foaming phenomena for a membrane bioreactor, Bioresour. Technol. 147 (2013) 184–192.
[15] M. DuBois, K.A. Gilles, J.K. Hamilton, P.A. Rebers, F. Smith, Colorimetric method for determination of sugars and related substances, Anal. Chem. 28 (1956) 350–356.
[16] O.H. Lowry, N.J. Rosebrough, A.L. Farr, R.J. Randall, Protein measurement with the Folin phenol reagent, J. Biol. Chem. 193 (1951) 265–275.
[17] I.S. Chang, S.O. Bag, C.H. Lee, Effects of membrane fouling on solute rejection during membrane filtration of activated sludge, Process Biochem. 36 (2001) 855–860.
[18] P.A. Veselind, Capillary suction time as a fundamental measure of sludge dewaterability, J. Water Pollut. Control Federation 60 (2) (1988) 215–220.
[19] M. Scholz, Review of recent trends in capillary suction time (CST) dewaterability testing research, Ind. Eng. Chem. Res. 44 (22) (2005) 8157–8163.
[20] G. Peng, F. Ye, Y. Li, Comparative investigation of parameters for determining the dewaterability of activated sludge, Water Environ. Res. 83 (7) (2011) 667–671.
[21] EN 14701-1, European Standard Characterization of Sludges – Filtration Properties – Part 1: Capillary Suction Time (CST), European Committee for Standardization, 2006.
[22] EN 14701-2, European Standard Characterization of Sludges – Filtration Properties – Part 2: Determination of the Specific Resistance to Filtration, European Committee for Standardization, 2006.
[23] G. Di Bella, D. Di Trapani, M. Torregrossa, G. Viviani, Performance of a MBR pilot plant treating high strength wastewater subject to salinity increase: analysis of biomass activity and fouling behaviour, Bioresour. Technol. 147 (2013) 614–618.
[24] G. Di Bella, N. Di Prima, D. Di Trapani, G. Freni, M.G. Giustra, M. Torregrossa, G. Viviani, Performance of membrane bioreactor (MBR) systems for the treatment of shipboard slops: assessment of hydrocarbon biodegradation and biomass activity under salinity variation, J. Hazard. Mater. 300 (2015) 765–778.
[25] K.N. Yogalakshmi, K. Joseph, Effect of transient sodium chloride shock loads on the performance of submerged membrane bioreactor, Bioresour. Technol. 101 (2010) 7054–7061.
[26] C. Cortés-Lorenzo, M. Rodríguez-Díaz, D. Sipkema, B. Juárez-Jiménez, B. Rodelas, H. Smidt, J. González-López, Effect of salinity on nitrification efficiency and structure of ammonia-oxidizing bacterial communities in a submerged fixed bed bioreactor, Chem. Eng. J. 266 (2015) 233–240.
[27] Ö. Karahan-Gül, N. Artan, D. Orhon, M. Henze, M.C.M. van Loosdrecht, Respirometric assessment of storage yield for different substrates, Water Sci. Technol. 46 (2002) 345–352.
[28] H. Hauduc, L. Rieger, T. Ohtsuki, A. Shaw, I. Takács, S. Winkler, A. Héduit, P.A. Vanrolleghem, S. Gillot, Activated sludge modelling: development and potential use of a practical applications database, Water Sci. Technol. 63 (2011) 2164–2182.
[29] M. Henze, C. Grady, W. Gujer, G. Marais, T. Matsuo, Activated Sludge Model No. 1, IAWPRC Task Group on Mathematical Modelling for Design and Operation of Biological Wastewater Treatment, IAWPRC Scientific and Technical Reports No. 1, 1987.
[30] D. Di Trapani, M. Capodici, A. Cosenza, G. Di Bella, G. Mannina, M. Torregrossa, G. Viviani, Evaluation of biomass activity and wastewater characterization in a

UCT-MBR pilot plant by means of respirometric techniques, Desalination 269 (2011) 190–197.
[31] F. Meng, H. Zhang, F. Yang, S. Zhang, Y. Li, X. Zhang, Identification of activated sludge properties affecting membrane fouling in submerged membrane bioreactors, Sep. Purif. Technol. 51 (2006) 95–103.
[32] J. Li, F. Yang, Y. Li, F.-S. Wong, H.C. Chua, Impact of biological constituents and properties of activated sludge on membrane fouling in a novel submerged membrane bioreactor, Desalination 225 (2008) 356–365.
[33] H. Lin, M. Zhang, F. Wang, Y. He, J. Chen, H. Hong, A. Wang, H. Yu, Experimental evidence for osmotic pressure-induced fouling in a membrane bioreactor, Bioresour. Technol. 158 (2014) 119–126.
[34] H. Lin, M. Zhang, F. Wang, F. Meng, B.-Q. Liao, H. Hong, J. Chen, W. Gao, A critical review of extracellular polymeric substances (EPSs) in membrane bioreactors: characteristics, roles in membrane fouling and control strategies, J. Membr. Sci. 460 (2014) 110–125.
[35] G.-P. Sheng, H.-Q. Yu, X.-Y. Li, Stability of sludge flocs under shear conditions: roles of extracellular polymeric substances (EPS), Biotechnol. Bioeng. 93 (2006) 1095–1102.
[36] S.J. Judd, C. Judd, Principles and applications of membrane bioreactors in water and wastewater treatment, 2nd edn., Elsevier, London, 2010.
[37] G. Mannina, G. Di Bella, G. Viviani, An integrated model for biological and physical processes in membrane bioreactors (MBR), J. Membr. Sci. 376 (2011) 56–69.
[38] M. Raynaud, J. Vaxelaire, J. Olivier, E. Dieudé-Fauvel, J. Baudez, Compression dewatering of municipal activated sludge: effects of salt and pH, Water Res. 46 (2012) 4448–4456.
[39] X.Y. Li, S.F. Yang, Influence of loosely bound extracellular polymeric substances (EPS) on the flocculation, sedimentation and dewaterability of activated sludge, Water Res. 41 (2007) 1022–1030.
[40] J. Houghton, J. Quarmby, T. Stephenson, Municipal wastewater sludge dewatering and the presence of microbial extracellular polymer, Water Sci. Technol. 44 (2) (2001) 373–379.
[41] J. Houghton, T. Stephenson, Effect of influent organic content on digested sludge extracellular polymer content and dewaterability, Water Res. 36 (2002) 3620–3628.
[42] X. Zhou, G. Jiang, T. Zhang, Q. Wang, G. Xie, Z. Yuan, Role of extracellular polymeric substances in improvement of sludge dewaterability through peroxidation, Short Commun. Bioresour. Technol. 192 (2015) 817–820.
[43] Y. Chen, H. Yang, G. Gu, Effect of acid and surfactant treatment on activated sludge dewatering and settling, Water Res. 35 (2001) 2615.